EUKARYOTIC CELL, Sept. 2008, p. 1530–1539 Vol. 7, No. 9
1535-9778/08/$08.00+0 doi:10.1128/EC.00080-08

Aspergillus fumigatus RasA Regulates Asexual Development and Cell Wall Integrity▽

Jarrod R. Fortwendel,† Kevin K. Fuller, Timothy J. Stephens, W. Clark Bacon, David S. Askew, and Judith C. Rhodes*

Department of Pathology and Laboratory Medicine, University of Cincinnati College of Medicine, 231 Albert Way, Cincinnati, Ohio 45267-0529

Received 3 March 2008/Accepted 11 June 2008

The Ras family of proteins is a large group of monomeric GTPases. Members of the fungal Ras family act as molecular switches that transduce signals from the outside of the cell to signaling cascades inside the cell. *A. fumigatus* RasA is 94% identical to the essential RasA gene of *Aspergillus nidulans* and is the Ras family member sharing the highest identity to Ras homologs studied in many other fungi. In this study, we report that *rasA* is not essential in *A. fumigatus*, but its absence is associated with slowed germination and a severe defect in radial growth. The Δ*rasA* hyphae were more than two times the diameter of wild-type hyphae, and they displayed repeated changes in the axis of polarity during hyphal growth. The deformed hyphae accumulated numerous nuclei within each hyphal compartment. The Δ*rasA* mutant conidiated poorly, but this phenotype could be ameliorated by growth on osmotically stabilized media. The Δ*rasA* mutant also showed increased susceptibility to cell wall stressors, stained more intensely with calcofluor white, and was refractory to lysing enzymes used to make protoplasts, suggesting an alteration of the cell wall. All phenotypes associated with deletion of *rasA* could be corrected by reinsertion of the wild-type gene. These data demonstrate a crucial role for RasA in both hyphal growth and asexual development in *A. fumigatus* and provide evidence that RasA function is linked to cell wall integrity.

Aspergillus fumigatus is an opportunistic fungal pathogen that causes a variety of diseases, ranging from allergic reactions to invasive pulmonary infection. The pathogenicity of this organism has been attributed to many factors, including thermotolerance, rapid growth of hyphae, and small conidial size (16). The conidia of *A. fumigatus*, considered the infective propagule, are ubiquitous in nature and are inhaled and cleared by immunocompetent hosts. However, in immunosuppressed patients, inhaled conidia survive and initiate growth. After germination and apical extension, the organism penetrates the pulmonary epithelium and vascular endothelium. In the vessel lumen, shear forces sever portions of the hyphae and deposit fungus-laden emboli in areas rich in microvasculature, leading to dissemination of the infection. Once dissemination has occurred, the mortality rate ranges from 30 to 85%, depending on the patient population (20).

The ability of the fungus to sense and respond to external stimuli is vital to the growth of the organism. Recently, considerable effort has been directed toward deciphering the signal transduction molecules involved in receiving and transmitting these external stimuli (19). The Ras superfamily, a large group of monomeric GTPase proteins, represents an important subset of these signaling molecules. Of the known Ras subfamily homologs, most act as molecular switches that transduce signals from the outside of the cell to signaling cascades inside the cell. Among the yeasts, Ras genes play roles in normal growth, and in some cases virulence, by contributing to a wide variety of cellular processes (reviewed in reference 41). Ras1p and Ras2p are the prototypical Ras proteins of *Saccharomyces cerevisiae*. The importance of *RAS2* in environmental sensing was first identified by its role in growth on nonfermentable carbon sources (13). Ras2p is also necessary for entry into the cell cycle during *S. cerevisiae* germination and, in combination with the Ras proteins Ras1p and Rsr1p, is required for completion of mitosis (12, 29). Deletion of *RAS2* in *S. cerevisiae* leads to slow growth rates, decreased intracellular cyclic AMP (cAMP) levels, accumulation of storage carbohydrates, and an increase in heat shock resistance, whereas expression of an activated form of Ras2p leads to hypersensitivity to stress, failure to arrest at G_1 upon nutrient limitation, and loss of viability at the stationary phase (14, 23, 37). The genome of a second model yeast, *Schizosaccharomyces pombe*, encodes only one Ras gene, *ras1*. *S. pombe ras1* is required for mating, since its deletion leads to a sterile phenotype (9). Strains lacking *ras1* also have abnormal cell shape and do not undergo polarized growth.

Ras homologs have been implicated in the growth and virulence of several yeast pathogens. In the human pathogen *Cryptococcus neoformans*, Ras1p was shown to be important for high temperature growth and, therefore, virulence (1). Deletion of *ras1* also leads to defects in mating and haploid filamentous growth. The contribution of Ca*RAS1* to morphology and virulence has been studied in *Candida albicans.* Ca*RAS1* deletion mutants are viable and capable of forming pseudohyphae but fail to form germ tubes and hyphae in the presence of serum (6). When a dominant active allele of *CaRAS1* is expressed, germination and hyphal growth are in-

* Corresponding author. Mailing address: Department of Pathology, University of Cincinnati, P.O. Box 670529, Cincinnati, OH 45267-0529. Phone: (513) 558-0130. Fax: (513) 558-2141. E-mail: Judith.rhodes@uc.edu.

† Present address: Department of Pediatrics, Duke University Medical Center, Research Drive, Durham, NC 27710.

▽ Published ahead of print on 7 July 2008.

duced in the absence of serum (6). Since Ca*RAS1* helps to regulate the dimorphic switch from yeast to hyphae, a phenotype closely linked to virulence, it is not surprising that the Ca*RAS1*-null strain has been shown to be avirulent in a mouse model. Finally, Ras activity has also been studied in the plant pathogen, *Ustilago maydis*. Deletion of *U. maydis ras2* results in a reduction in filamentous growth, leading to a rounded-cell phenotype (18). These cells, due to lack of filamentous growth, are nonpathogenic.

To date, the functions of Ras among the filamentous fungi have been limited to the study of dominant-active and dominant-negative mutants, normally expressed in a wild-type (wt) Ras background. Isolation of a viable deletion mutant in homologs of RasA has never been reported among the filamentous fungi, suggesting either that RasA activity is essential or that deletion leads to such severe growth inhibition that isolation and characterization is impractical. Although a *rasA* deletion mutant of *Aspergillus nidulans* has never been isolated, high-level expression of a dominant-active RasA leads to precocious germination and inhibits asexual development (25, 34). Similar results were seen with expression of dominant-active RasA in *A. fumigatus* (8). Expression of either a dominant-active or dominant-negative *Penicillium marneffei rasA* allele results in a delay in germination and abnormal isotropic growth (2). In addition, expression of an activated *ct-Ras* allele in the plant pathogen, *Colletotrichum trifolii*, affects polarized growth and causes reduced conidiation, whereas dominant-negative *ct-Ras* expression decreases germination and growth rates (38). These data, taken together, indicate that RasA homologs of the filamentous fungi play important, conserved roles in germination and the polarized growth of hyphae.

We report here the first successful isolation and characterization of a *rasA* deletion mutant in a filamentous fungus. Unlike the *rasA* homologs found in *A. nidulans*, *P. marneffei*, and *C. trifolii*, the *rasA* gene of *A. fumigatus* was nonessential, although deletion led to severe growth defects characterized by severely malformed hyphal and colony morphologies and nuclear aberrancies. In addition, a surprising phenotype of increased sensitivity to cell wall stress was identified in the Δ*rasA* mutant. These data demonstrate that RasA is necessary for normal germination and development in *A. fumigatus* and provide evidence that RasA contributes to cell wall integrity.

MATERIALS AND METHODS

Reagents. Caffeine (C8960), fluorescent brightener 28 (F3543), Congo red (C6277), sodium dodecyl sulfate [SDS] (L4390), cAMP (A6885), dibutyryl cAMP (D0627), aniline blue (M5528), glucosamine (G1514), yeast glucan (G5011), and propidium iodide (P5264) were obtained from Sigma and dissolved in sterile, distilled water. Nikkomycin Z (N8028; Sigma) was dissolved in 100% ethanol, and cyclosporine (C1832; Sigma) was dissolved in dimethyl sulfoxide (DMSO). Fungin (ant-fn-1) was purchased from Invivogen. All reagents were stored at −20°C until use.

***A. fumigatus* strains and growth conditions.** *A. fumigatus* strain H237 is a clinical isolate and served as the wt strain for these studies. Strain H237, the Δ*rasA* mutant strain, and the Δ*rasA*+*rasA* reconstituted strain (described below) were maintained on and harvested from *Aspergillus* minimal medium (AMM) agar plates, modified to contain 10 mM ammonium tartrate as a nitrogen source, and no supplement solution (3). Submerged cultures for determination of biomass and germination rates were grown in AMM broth as indicated. Germination experiments were performed by inoculating AMM broth with 10^5 conidia/ml, followed by incubation over coverslips at 37°C. At the indicated times, coverslips were removed from the culture, and the number of conidia with visible germ tubes were counted. To visualize morphological changes in response to cell wall stress, AMM broth was inoculated with 10^5 conidia/ml and incubated on coverslips for 16 h with the indicated concentrations of cell wall stress agents. At the end of 16 h, coverslips were removed and mounted for analysis using an Olympus BH-2 microscope. Determination of total biomass in liquid culture was performed by inoculating 10^4 conidia into preweighed, sterile test tubes containing 5 ml of AMM broth, followed by incubation at 37°C with shaking at 250 rpm. After 24 and 48 h of incubation, the tubes were frozen in an ethanol-dry ice bath and then lyophilized for 24 h before a final weight was recorded. For growth rate analysis on solid medium, 10^4 conidia were spotted in the center of AMM agar plates, followed by incubation at specified temperatures. The change in colony diameter was recorded every 24 h for up to 5 days. Growth rates were based on the change in diameter (in millimeters) between 24 and 48 h. All of these experiments were performed in triplicate. For the determination of conidial yield on osmotically stabilized medium, 100 μl of 10^5 conidia/ml were spread onto AMM agar plates with or without the indicated osmotic stabilizer. After 5 days of incubation at 37°C, 5 ml of sterile water was poured over the plate, and conidia were harvested by using a sterile swab. Harvested conidia from each strain were then filtered and counted on a hemacytometer.

In order to compare the microscopic morphologies of the conidiophores, cultures of the members of the *rasA* isogenic set were grown up on AMM, osmotically stabilized AMM (OSM), yeast glucose, and osmotically stabilized yeast glucose agars. Media were osmotically stabilized by the addition of 1.2 M sorbitol. The morphology of mature conidiophores, defined as those bearing conidia, was examined at 24 and 48 h for the wt and complemented strains and after 72 and 96 h for the mutant, because of the delay in germination.

***rasA* deletion and reconstitution constructs.** A deletion of the entire *rasA* coding region was achieved by use of double homologous recombination after transformation of protoplasts, as previously described (8). First, the primers rasA L arm-F and rasA L arm-R were designed to amplify a 3-kb region upstream of the predicted *rasA* translation start site. Second, the primers rasA R arm-F and rasA R arm-R were used to amplify a 2-kb region downstream of the predicted *rasA* stop codon. All primer sequences are provided in Table 1. These PCR fragments were then separately cloned into pGEM-T Easy (Promega) and confirmed by sequencing (University of Cincinnati DNA Core Facility). A 1.8-kb NdeI/SacI fragment of the downstream arm was then cloned into the NdeI/SacI sites of the vector containing the upstream arm, forming a new construct that contained the left flank directly connected to the right flank. To complete the construct, a hygromycin resistance cassette was then subcloned from pAN7-1 as an XhoI/XbaI fragment into SpeI/SalI restriction sites that existed at the junction of the left and right flanking regions (30). The nonlinearized deletion construct was then transformed into *A. fumigatus* protoplasts and plated under hygromycin

TABLE 1. Primers used in this study

Gene	Primer	Sequence (5′–3′)
rasA	rasA L arm-F	GCCGAAGTAATGCTCATG
rasA	rasA L arm-R	CACGGCGAAGTCTAGGTTG
rasA	rasA R arm-F	GTCGACGTTGCTTTACACGG
rasA	rasA R arm-R	CAGGCCCTCCGAGATGGG
rasA	rasA Comp-F	GTCTCTTATCATTATTGG
rasA	rasA Comp-R	GATAATGCGGCCGCGTAAAGC AACGTCGACCC
rasA	rasA RT-PCR-F	ATGGCTTCAAAGTTCC
rasA	rasA RT-PCR-R	TAAAGCAACGTCGACCC
fksA	fksA-F	ATTGCAGCAGCGGCCATTCAGC
fksA	fksA-R	CGCTCTCAACTGGCTCAAATCC
gpdA	gpdA-F	TCATCAACGACAAGTTCGGC
gpdA	gpdA-R	ACAACACGGCGAGAGTAACC
modA	modA-F	TCGGTGATGAGCCCTATACC
modA	modA-R	CAGCAAGACGCATCTGGACTTC
mpkA	mpkA-F	ATCTGCGATTTCGGTTTGGC
mpkA	mpkA-R	TGTCGTCGGGCAGGTGGGCTC
pkaC1	pkaC1-F	CTCAATCGTGTCAGGCATCC
pkaC1	pkaC1-R	CCAGTCGCTTTGTCAAATCC
pkaC2	pkaC2-F	GGCTGGCGAAATTCAAAGAC
pkaC2	pkaC2-R	GCTGCCCAACCAAAAACTCG
pkaR	pkaR-F	GCTCCTTTGGTGAACTAGCC
pkaR	pkaR-R	TCTCATAATATCCTCCACAG
sakA	sakA-F	AGAACTGCTTGGGACTCCGCC
sakA	sakA-R	CACGCCTCCTTCCATGAGCACC

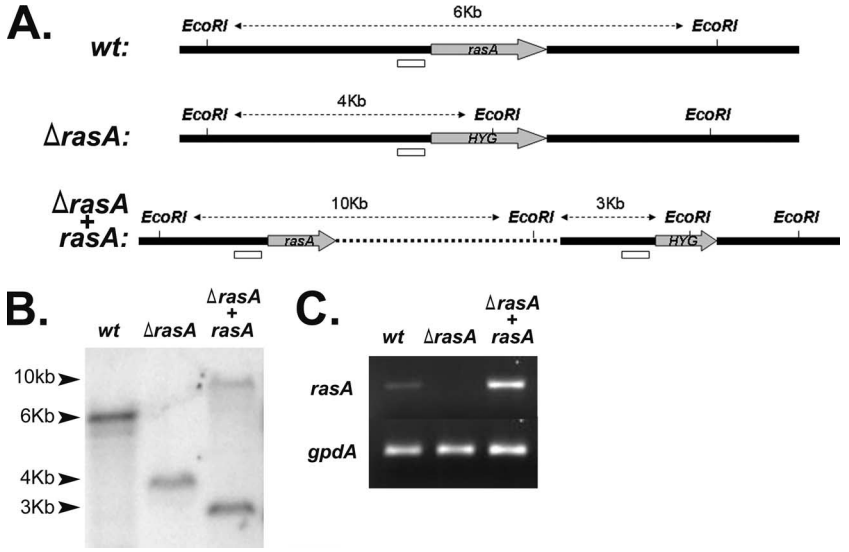

FIG. 1. Deletion of *A. fumigatus rasA*. (A) Schematic of the *rasA* genomic locus from the wt, deletion (Δ*rasA*), and reconstituted (Δ*rasA*+*rasA*) strains. Probes used for Southern blot application are shown as small white boxes, and the relative positions of the EcoRI restriction sites are indicated. The dotted line shown in the Δ*rasA*+*rasA* strain represents plasmid sequence inserted during integration of the complementation construct. (B) Genomic Southern blot of wt, Δ*rasA*, and Δ*rasA*+*rasA* strains digested with EcoRI. (C) RT-PCR of the isogenic set using *rasA* gene-specific primers. Amplification control is *A. fumigatus gpdA*.

selection (267 μg/ml). Plates were incubated at 37°C and monitored for 3 weeks. Hygromycin-resistant colonies were isolated to new media as they arose.

The Δ*rasA* mutation was reconstituted by incorporation of a single copy of wt *rasA* locus adjacent to the deleted locus to make the reconstituted strain called the Δ*rasA*+*rasA* strain. The plasmid was built as follows. The primers rasA Comp-F and rasA Comp-R were used to PCR amplify a 2-kb region containing the *rasA* locus plus 1 kb of the 5′ flank from the *A. fumigatus* genome. This PCR fragment was cloned in PCR-TOPO 2.1 (Invitrogen) and sequenced (University of Cincinnati DNA Core Facility). To finalize the construct, this *rasA* fragment was excised from PCR-TOPO 2.1 as a BamHI-NotI fragment and cloned into the BglII-NotI restriction sites of pTPP. Vector pTPP was constructed by subcloning the phleomycin resistance cassette from pBCphleo (Fungal Genetics Stock Center) as a SalI-HindIII fragment into pSL1180 (Pharmacia) digested with XhoI-HindIII. To complete the pTPP vector, the *trpC* terminator from pAN7-1 was subcloned as a SacII-SacI fragment, upstream of the newly cloned phleomycin resistance cassette. The addition of the *trpC* terminator sequence is to act as a terminator sequence for any gene cloned into pTPP. The final *rasA* reconstitution construct was then transformed into Δ*rasA* protoplasts and plated under phleomycin selection (125 μg/ml). Plates were incubated at 30°C and monitored for 1 week. Phleomycin-resistant colonies were isolated to new media as they arose.

Southern blot and RT-PCR analyses. DNA and RNA were extracted as previously described (8). In order to confirm that *rasA* deletion and reconstitution was achieved, Southern blots were performed by using EcoRI to digest the genomic DNA. Blots were probed with a fragment of the *rasA* promoter sequence, bp −500 to −1 from the *rasA* translation start site. A graphical representation of this deletion and reconstitution scheme is provided in Fig. 1. For reverse transcription-PCR (RT-PCR) analysis of the *rasA* transcript levels, mRNA was isolated from the isogenic set by using the mRNA Catcher PluS 96-well plate (Invitrogen). Isolated mRNA was quantitated, and equal amounts were used for PCR amplification. PCR was carried out using the *rasA*-specific primers rasA RT-PCR-F and rasA RT-PCR-R.

Relative expression levels by RT-PCR. Hyphae from each member of the isogenic set were harvested from AMM after 21 h of incubation at 37°C and 200 rpm and used as the starting material for RNA isolation (RNeasy; Qiagen). RT-PCR to determine transcript levels of *fksA*, *modA*, *mpkA*, *sakA*, *pkaC1*, *pkaC2*, and *pkaR* was performed on first-strand cDNA (Superscript III; Invitrogen) made from the extracted RNA after treatment with DNase (RQ1 DNase; Qiagen). The Sybr green-stained band intensity was normalized to *gpdA*, as previously described (27). Mean ratio values were determined from three independent experiments, and analysis of variance was used to analyze differences among the members of the isogenic set for a given experimental gene. Controls in which reverse transcriptase was omitted were performed with each primer-sample combination. All of the primers are listed in Table 1.

Staining of nuclei and the cell wall. Staining of nuclei, septa, and cell walls was performed by a modification of previously described protocols (21, 26). In short, freshly harvested conidia were incubated on coverslips immersed in AMM broth. At specified times, coverslips were removed, washed twice in 50 mM PIPES (pH 6.7) and fixed in 3 ml of fixative solution (8% formaldehyde in 50 mM PIPES [pH 6.7], 25 mM EGTA [pH 7.0], 5 mM $MgSO_4$, and 5% DMSO) for 30 min. After fixation, the coverslips were washed twice for 10 min in 50 mM PIPES (pH 6.7), RNase (0.1 mg/ml) was added, and the samples were incubated at 37°C for 1 h. The coverslips were then washed twice for 10 min in 50 mM PIPES (pH 6.7) and inverted onto 0.5 ml of freshly made staining solution (propidium iodide [12.5 μg/ml; Sigma] and fluorescent brightener 28 [0.4 μg/ml; Sigma] in 50 mM PIPES [pH 6.7]) for 5 min at room temperature. Finally, the coverslips were washed twice for 10 min in 50 mM PIPES (pH 6.7) and mounted in 50% glycerol. Fluorescence microscopy was performed on an Olympus AX80 microscope using a digital camera equipped with a DAPI (4′,6′-diamidino-2-phenylindole)/fluorescein isothiocyanate/TRITC (tetramethyl rhodamine isothiocyanate) triple cube filter. Digital images were analyzed using Spot Advanced and Photoshop 7.0 software. Bright-field and differential interference contrast analysis were performed on an Olympus BH-2 microscope.

CMFDA fungal growth assay. The chloromethyl-fluorescein diacetate (CMFDA) assay for fungal growth was performed, with slight modification, as previously described (44). Into a masked, 96-well optical bottom plate (Nunc), 10^5 conidia were added per well in 50 μl of AMM. The final assay volume of 100 μl was made up with 50 μl of AMM containing the various cell wall stress agents at a 2× the assay concentration. Control wells contained various concentrations of cell wall stress agents with no conidial inoculum. After 16 to 18 h of incubation at 37°C, 100 μl of 5 μM CMFDA in a buffer containing 110 mM glucose, 10 mM NaCl, and 10 mM HEPES (pH 7.2) was added to each well, and the plate was incubated as before for 1 h. Fluorescence was measured by using a FLUOstar Optima plate reader with a 485-nm excitation filter and a 520-nm emission filter. Each strain and treatment was loaded in triplicate for each experiment, and all experiments were performed three times. The results are presented as a percentage of CMFDA fluorescence calculated by comparison of total fluorescence of treated wells versus untreated wells.

Growth assays with pharmacologic agents. Plates of AMM containing graded concentrations of cyclosporine or the DMSO vehicle were inoculated with 10^4 conidia harvested from each member of the *rasA* isogenic set. Plates were incubated at 37°C for 72 h.

Conidia (10^4) of each member of the isogenic set were inoculated into wells in a 24-well plate containing AMM and OSM. One series of wells contained 10 mM

cAMP, and a second series contained 10 mM dibutyryl cAMP. The plates were incubated for 48 h at 37°C.

Cell wall assays for β-glucan. Flasks of AMM were inoculated with 10^5 conidia per ml and incubated at 37°C and 200 rpm for 18 to 21 h. Hyphae were harvested by centrifugation, washed, and processed for β-glucan content by using a modification of an aniline blue dye procedure (15, 33). Approximately 5 mg of lyophilized hyphae was used as the starting material. Yeast glucan was used as the standard. The fluorescence was read on a FLUOstar Optima, using an excitation wavelength of 405 nm and an emission wavelength of 520 nm.

RESULTS

Deletion of *A. fumigatus rasA*. Previous studies in filamentous fungi used dominant-active or dominant-negative alleles of RasA to study RasA function. In the present study we sought to gain insight into RasA function by replacing the entire *rasA* coding region with a dominant selectable marker encoding hygromycin resistance (Fig. 1A). In order to ensure that the Δ*rasA* mutant phenotypes were the result of *rasA* deletion alone, a *rasA* complementation construct was introduced via a single crossover integration in the *rasA* promoter region (Fig. 1A). Deletion and reconstitution of the *rasA* coding sequence was verified by Southern blot analysis (Fig. 1B). Genomic DNA from each strain of the isogenic set was digested with EcoRI and hybridized with a ^{32}P-labeled probe from the *rasA* promoter sequence. The wt and deletion strains yielded a ~6-kb and a ~4-kb band, respectively, and the complemented strain (Δ*rasA*+*rasA*) produced a 3-kb band corresponding to the original deletion locus and a 10-kb band from integration of the complementation construct. These band sizes were as predicted based on the introduction and/or deletion of EcoRI restriction sites within the region. As further confirmation, RT-PCR using gene-specific primers confirmed the loss, and reappearance, of *rasA* mRNA in the Δ*rasA* and Δ*rasA*+*rasA* strains, respectively (Fig. 1C).

Loss of RasA causes severe growth inhibition. When grown on solid media, the Δ*rasA* mutant formed a tightly compact colony with limited capacity for radial outgrowth, accompanied by nearly absent conidiation (Fig. 2A and Fig. 3). The diameter of the Δ*rasA* mutant colony was only ca. 50% of the size of the wt colony after the first 48 h of growth at 30 or 37°C. No further substantial outgrowth was noted for the mutant over the next 72 h of incubation at 37°C. When the coding region of *rasA* was reinserted into the genome of the deletion mutant, both the growth and conidiation defects were complemented. Because this severe reduction in colony diameter is similar to the phenotype of the calcineurin catalytic subunit deletion mutant, the sensitivity of Δ*rasA* to the calcineurin inhibitor cyclosporine was examined (Fig. 3). The ability of the mutant to respond to cyclosporine suggested that the calcineurin pathway was still intact in the Δ*rasA* mutant (4, 35).

Interestingly, growth on media containing 1.2 M sorbitol remediated the reduced conidiation phenotype of the Δ*rasA* strain (Table 2) but did not ameliorate the reduced Δ*rasA* radial growth (Fig. 3). Although improved conidiation could be achieved by supplementation of the medium with either organic or inorganic osmotic stabilization compounds, osmotic stabilization of the medium did not prevent the appearance of abnormal conidiophore morphology, such as a "double-vesicle" head at the tip of the conidiophore (Fig. 4D). Abnormal morphology, including branched, rudimentary, or septate conidiophores. was detected in 30 to 35% of the Δ*rasA* conidiophores isolated from osmotically stabilized media, whereas both the wt and the Δ*rasA*+*rasA* strains showed at most 20% abnormal (septate stalks only) conidiophores on the same medium (Fig. 4). Even in the most normal-appearing mutant conidiophores, the phialides were notably blunted or rounded at the tip, rather than being the normal, "bowling pin" shape, as seen in the wt and complemented strains.

Exogenous cAMP does not complement the ΔrasA growth defect. Because some of the morphological and developmental phenotypes seen in *C. albicans* and *C. neoformans* can be remediated by the addition of exogenous cAMP, the growth of the *rasA* isogenic set was compared on AMM with or without 10 mM cAMP or dibutyryl-cAMP (1, 17, 24). Neither of the cyclic nucleotides, either tested alone or in combination with an osmotic stabilizer, was able to restore wt phenotypic features to the *rasA* deletion mutant (Fig. 3 and data not shown).

Deletion of *rasA* impairs germination and hyphal development. In medium containing glucose as the sole carbon source, the Δ*rasA* mutant displayed decreased germination rates, requiring nearly 3 h longer than wt or Δ*rasA*+*rasA* strain to reach 100% germination (Fig. 2B). However, Δ*rasA* conidia were 100% viable (data not shown). In liquid culture, the total hyphal mass of the Δ*rasA* mutant was greatly decreased after 24 and 48 h of growth, even after correcting for the germination delay (Fig. 2C). No difference in biomass accumulation was noted between the wt and reconstituted strains. Microscopic examination of hyphae formed in submerged culture (Fig. 5) revealed striking morphological defects in the Δ*rasA* mutant. After 16 h of submerged growth, Δ*rasA* hyphae displayed a stunted phenotype with frequent changing of the axis of polarity. In contrast to wt *A. fumigatus*, which was able to maintain a single, constant growth axis over 50 μm of growth, the Δ*rasA* hyphae changed their axis of growth polarity as many as seven times (Fig. 5). Mutant hyphae were more than two times the diameter of wt hyphae and appeared more refractile under light microscopy. These abnormal hyphal development characteristics were not seen in the wt or reconstituted strains under similar conditions.

RasA regulates nuclear morphology and distribution. Because alteration of RasA activity has been shown to cause aberrant mitotic events in both *A. fumigatus* and *A. nidulans*, nuclear division and distribution was examined in the Δ*rasA* mutant (8, 34). After 16 h of culture in YG medium, wt hyphae, stained with propidium iodide and calcofluor white, displayed an average of five to seven evenly spaced nuclei per subapical compartment (Fig. 6). These data are in keeping with the previously reported averages for *A. fumigatus* (21). In contrast, hyphae from the Δ*rasA* strain contained many variably sized nuclei, unevenly distributed throughout the hyphae (Fig. 6).

Growth inhibition due to RasA deletion is not enhanced at elevated temperatures. In *C. neoformans*, growth inhibition of the *RAS1* deletion strain worsens upon incubation at 37°C, and the mutant fails to grow at 39°C, implying that the effects of deletion and high temperature are additive (1). To test for this phenotype in the *A. fumigatus rasA* mutant, conidia from the wt, Δ*rasA*, and Δ*rasA*+*rasA* strains were inoculated onto AMM and allowed to grow for 48 h at 30 or 37°C. The Δ*rasA* mutant developed a colony diameter roughly 50% that of the wt and

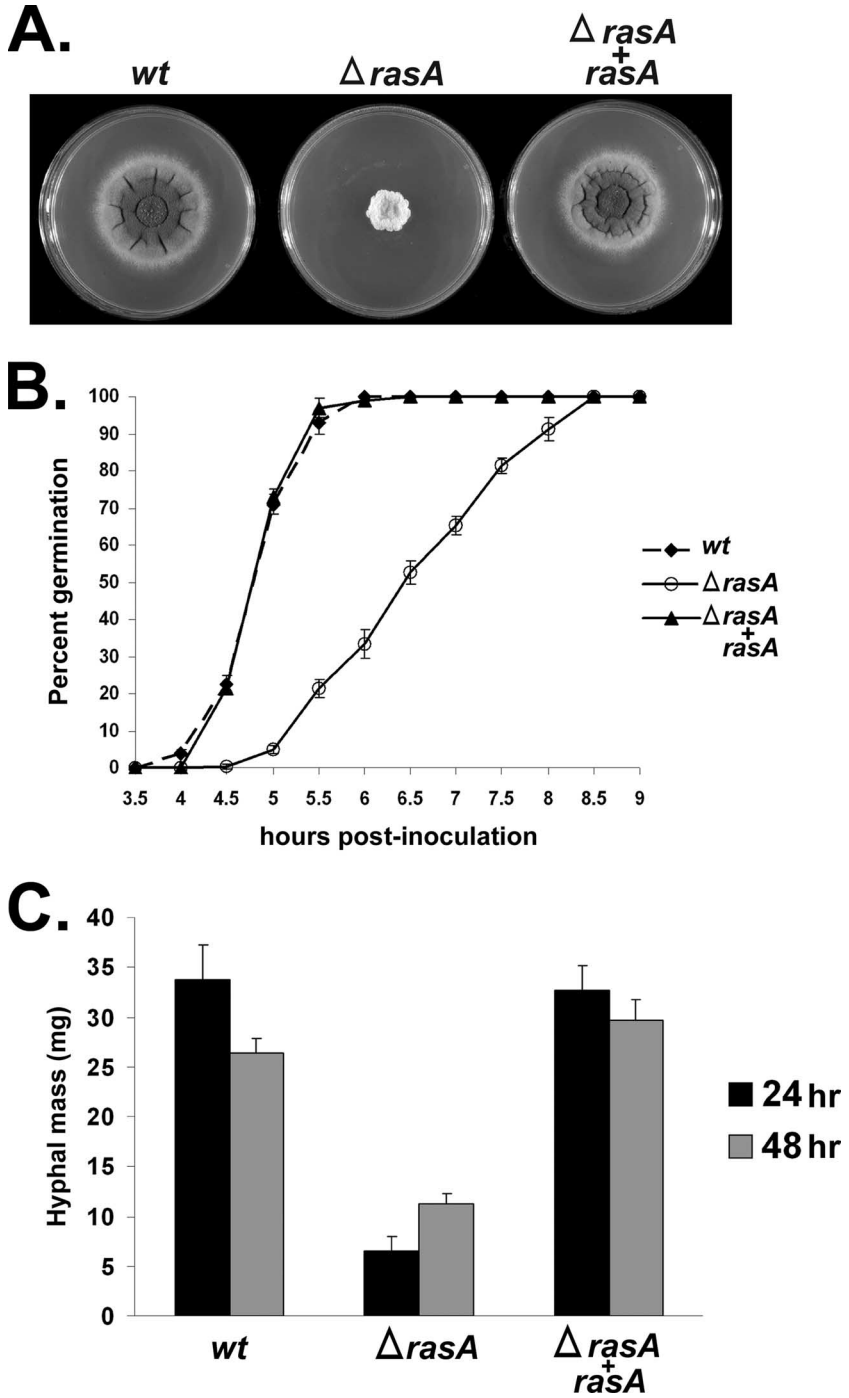

FIG. 2. Deletion of *rasA* affects colony morphology and radial growth. (A) Colony morphology of the *A. fumigatus* wt, Δ*rasA*, and Δ*rasA*+*rasA* strains. Equal numbers of conidia were inoculated and allowed to grow for 48 h at 37°C on AMM. (B) Germination rates of the isogenic set. Conidia (10^4) from each strain were inoculated onto coverslips and submerged in YG media at 37°C. The percent germination was scored as the number of conidia producing a visible germ tube among 100 total enumerated conidia. (C) Comparison of total biomass from the isogenic set. Each strain was grown for 24 or 48 h at 37°C in YG, and the total biomass was determined as described in Materials and Methods. All experiments were performed in triplicate. Measurements and error bars represent the mean ± the standard deviation (SD).

the Δ*rasA*+*rasA* strains at 48 h at either 30 or 37°C. The Δ*rasA* mutant displayed a 74% reduction in radial growth rate when incubated at 37°C and a 77% reduction at 30°C (37°C growth rates: wt = 0.61 mm/h, Δ*rasA* = 0.16 mm/h, Δ*rasA*+*rasA* = 0.59 mm/h; 30°C growth rates: wt = 0.35 mm/h, Δ*rasA* = 0.08 mm/h, Δ*rasA*+*rasA* = 0.42 mm/h). These data indicate that the growth inhibition caused by loss of RasA is not enhanced at high temperatures and that RasA activity is not essential for the unique thermotolerance of this filamentous fungus, at least under the conditions tested.

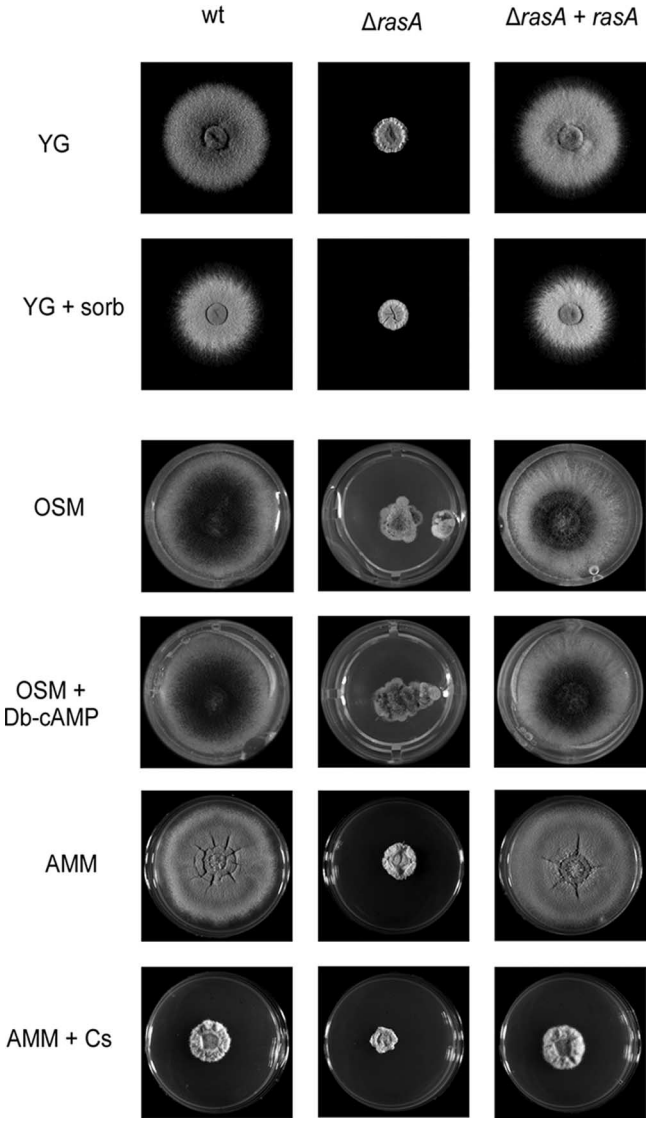

FIG. 3. Deletion of *rasA* causes restricted radial growth. Colonies of the members of the *rasA* isogenic set were compared after 48 h of incubation at 37°C. The addition of 1.2 M sorbitol did not correct the radial growth defect (YG versus YG+sorb), but conidiation was restored. The addition of exogenous cAMP (as dibutyryl-cAMP [Db-cAMP]) to OSM did not remediate the growth phenotype, even in the presence of sorbitol (OSM+DbcAMP). Inhibition of the calcineurin pathway by the addition of 75 μM cyclosporine (Cs) to AMM resulted in radial growth inhibition of all members of the *rasA* isogenic set, implying that calcineurin is active in the *rasA* deletion mutant.

Loss of *rasA* increases resistance to digestion and sensitivity to cell wall and membrane stress. Cell wall-degrading enzymes can be used to liberate *A. fumigatus* protoplasts from germling cells. However, several preparations of cell wall-degrading enzymes that are typically used to protoplast *A. fumigatus* hyphae were not effective with the Δ*rasA* strain (Table 3). For example, use of a mixture of driselase, lyticase, and β-D-glucanase yielded no protoplasts from the Δ*rasA* strain (26). In fact, even at concentrations of protoplasting enzymes that were double those effective with the wt, no protoplast formation was seen with the Δ*rasA* mutant. Vinoflow FCE, when used as described for protoplast generation with *Aspergillus*, resulted in extremely low protoplast yield (http://www.fgsc.net/Aspergillus/Vinoflow%20protoplasting.pdf). Adequate generation of protoplasts from the Δ*rasA* deletion mutant was only achieved by digesting germlings with the highly active cell wall-degrading enzyme preparation Novozyme 234. Because these data suggest differences in the cell wall composition and/or architecture of the Δ*rasA* mutant compared to the wt, we next measured the β-glucan content in the cell walls and the steady-state message levels of *fksA*, the β-glucan synthetase. No significant differences in glucan concentration were detected among the members of the *rasA* isogenic set, with all three isolates averaging between 2.8 and 3.9 μg of glucan per mg of dry weight. Likewise, message levels for *fksA* among the members of the isogenic set were not significantly different (see Fig. 9).

Since the Δ*rasA* mutant did not show quantitative differences in glucan content, the sensitivity to agents known to perturb the cell wall stability of fungi, manifested as the inhibition of growth and/or abnormal morphology, was tested. When incubated at 37°C in the presence of 75 μg of Congo red/ml, the growth of the Δ*rasA* mutant was severely inhibited, forming large swollen cells with no polarized growth axis (Fig. 7). Similar aberrant morphology was noted in the presence of 1 μg of Nikkomycin Z/ml; the Δ*rasA* mutant formed large, swollen "ballooned" cells (Fig. 7). At each of these concentrations, the wt and Δ*rasA*+*rasA* strains displayed minimal growth abnormalities, consisting of swollen cells interspersed with normal hyphal strands. Interestingly, aberrant phenotypes produced in the Δ*rasA* mutant by treatment with each stressor could be remediated, at least partially, by the addition of 1.2 M sorbitol to the growth medium (Fig. 7). In the presence of increasing amounts of SDS, the Δ*rasA* mutant displayed a sharp decrease in growth, as measured by the CMFDA fungal growth assay. However, the wt and Δ*rasA*+*rasA* strain were able to resist slightly higher levels of SDS (Fig. 8A and data not shown). A similar pattern was obtained after treatment with caffeine and Fungin. The Δ*rasA* mutant displayed high sensitivity to very low levels of Fungin (0.75 μg/ml) compared to the wt and complemented strains, and growth was reduced in 3 mM caffeine for Δ*rasA* (Fig. 8B and C, respectively). The inhibition of growth occurred in a concentration-dependent manner for SDS, caffeine, and Fungin alike. Despite the phenotypic differences in response to cell wall perturbation seen in the Δ*rasA* mutant, transcriptional responses were not detected in mitogen-activated protein kinases (MAPKs) involved in cell wall integrity (*mpkA* and *sakA*), in the Rho GTPase involved in control of growth polarity (*modA*), or in protein kinase A

TABLE 2. Conidial yield on osmotically stabilized media[a]

Treatment	Conidial yield (conidia/ml)	
	Wild type	Δ*rasA* mutant
No treatment	2.3×10^7	3.2×10^2
1.2 M sorbitol	8×10^7	4×10^7
1.2 M sucrose	7.6×10^7	2.9×10^7
1.2 M KCl	7.0×10^7	8.2×10^6
1.2 M NH_4Cl	6.4×10^7	2.5×10^6

[a] Conidia were harvested from plates incubated for 5 days at 37°C.

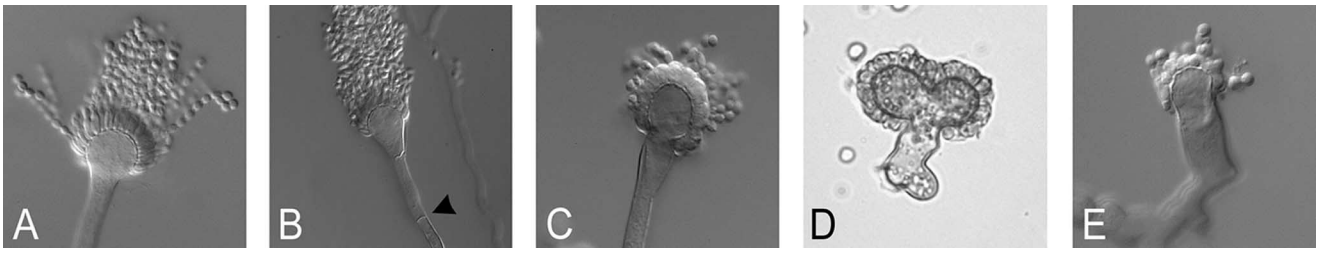

FIG. 4. Microscopic morphology of wt and Δ*rasA* conidiophores on osmotically stabilized medium. Conidiophores from the wt (A and B) and Δ*rasA* (C to E) strains grown on YG plus 1.2 M sorbitol for 2 days at 37°C are shown. Note the septated conidiophore in panel B (arrowhead), seen in 15 to 20% of wt and Δ*rasA*+*rasA* conidiophores on sorbitol containing medium. A minority of mutant conidiophores were relatively normal (C), but even those showed blunted phialides. Many mutant conidiophores were branched (D) or bizarre and rudimentary (E). Conidiophores from the Δ*rasA*+*rasA* strain (not shown) were indistinguishable from the wt. All were photographed at 400× using differential interference contrast (panels A to C and panel E) or bright-field microscopy (panel D).

(PKA), which is involved in oxidative stress responses (*pkaC1*, *pkaC2*, and *pkaR*) (Fig. 9 and data not shown).

DISCUSSION

The data provided here reveal roles for *A. fumigatus* RasA in many stages of the asexual growth cycle, including the development of proper cell wall integrity; the timing of germination, hyphal morphology, and growth; the nuclear distribution; and asexual development. There is ample precedent to suggest that many of these roles for Ras are conserved among the fungi. Although the molecular mechanisms by which Ras imparts this developmental control have been well studied in yeast, there are few data for the filamentous fungi. Such studies have been limited, at least in part, by the essential nature of *ras* genes among this group of fungal organisms. Surprisingly, the studies described here show that *rasA* is nonessential in *A. fumigatus.*

Deletion of *A. fumigatus rasA* led to a decrease in germination and radial growth rates and severe defects in hyphal morphology, with all phenotypes indicative of aberrancies in polarized growth. Although contributions of Ras activity to polarized growth processes have been noted in several fungi, exploration of the molecular mechanisms has been pursued primarily in yeast. For example, the conserved Ras/Cdc42/MAPK pathway and the Ras/PKA pathway have been implicated as possible polarity regulators in *S. cerevisiae*, *C. albicans*, *C. neoformans*, and *U. maydis* (1, 17, 18, 22). In contrast, the only mediator of Ras activity known to control polarized growth of the yeast *S. pombe* is the Cdc42 signaling pathway. Our data suggest that *A. fumigatus*, like some other filamentous fungi, is more similar to *S. pombe*, since growth on exogenous cAMP, even in the presence of 1.2 M sorbitol, did not remediate the Δ*rasA* growth and development phenotypes (Fig. 3). This is in contrast to what has been reported in *C. albicans* and *C. neoformans*. In *C. albicans*, the homozygous deletion of Ca*RAS* leads to a profound defect in the morphological transition to filamentous growth, which can be reversed by the addition of exogenous cAMP (17). Likewise, in *C. neoformans*, the mating defect in the Δ*ras1* strain is, at least partially, remediated by exogenous cAMP (1). The failure of cAMP to remediate the Δ*rasA* phenotypes in *A. fumigatus* is consistent with RasA signaling through ModA (CDC42) and MAPK pathways rather than through PKA. Indeed, in *A. nidulans*, Ras and PKA have also been shown to control germination processes through separate mechanisms (7).

In the model yeast *S. cerevisiae*, Ras also signals through Cdc42 and MAPK pathways to control pseudohyphal growth, and this interaction is mediated by 14-3-3 scaffold proteins (32). In *S. pombe*, signaling through the Ras/Scd1 (a guanine exchange factor for Cdc42) pathway is believed to be important for actin and microtubule assembly, both of which are important for proper polarized growth (28). In fact, attempts to obtain null mutants of Cdc42 in the filamentous fungi *Ashbya gossypii* and *P. marneffei* have been unsuccessful, suggesting that such deletions are lethal (2, 42). However, in filamentous

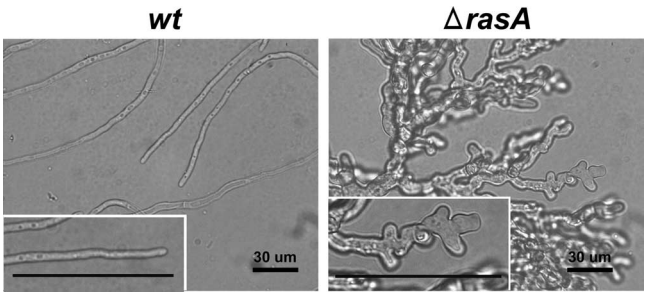

FIG. 5. Deletion of *rasA* affects hyphal morphology. wt and Δ*rasA* hyphae grown for 16 h at 37°C in liquid AMM are shown. Higher-magnification images, shown as insets, highlight the aberrant polarized growth of the Δ*rasA* mutant. Scale bar of inset, 50 μm.

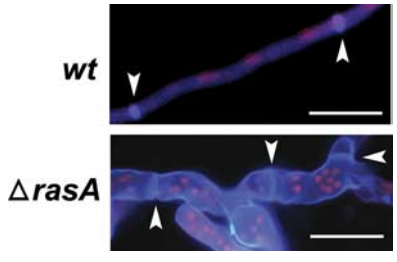

FIG. 6. Deletion of *rasA* affects nuclear distribution in *A. fumigatus*. Fluorescent images of the wt and Δ*rasA A. fumigatus* strains grown for 16 h at 37°C and 250 rpm are shown. Arrowheads indicate the presence of septa. All strains were fixed as described in Materials and Methods and stained with propidium iodide to visualize nuclei and calcofluor white to visualize the cell wall. Note the relative chitin-bright staining of the Δ*rasA* cell wall. Scale bar, 20 μm.

TABLE 3. Total protoplast yield[a]

Strain	Total no. of protoplasts[b]			
	Enzyme mix 1	Enzyme mix 2	Vinoflow FCE (64 mg/ml)	Novozyme 234[c]
Wild type	5.2×10^7	7.5×10^7	1.8×10^8	1.2×10^8
Δ*rasA* mutant	ND	ND	3.6×10^4	4.5×10^7

[a] Protoplasts were harvested from germlings incubated in the different protoplasting enzyme mixtures after 1 h of incubation at 37°C with shaking at 75 rpm.
[b] Enzyme mix 1: 16 mg/ml, β-D-glucanse; 10 mg/ml, driselase; 162.5 mg/ml, lyticase. Enzyme mix 2: 32 mg/ml, β-D-glucanase; 20 mg/ml, driselase; 325 mg/ml, lyticase. ND, none detected.
[c] 2 mg/40 mg hyphae.

fungi, as in higher eukaryotes, there is redundancy in the pathway in the form of Rac GTPases. Therefore, it is perhaps not surprising that studies in *A. nidulans* have illustrated redundant and overlapping roles of the two GTPases, which allows the deletion of CDC42 (*modA*) in this filamentous fungus (40). Interestingly, in addition to a markedly restricted radial growth phenotype in *A. nidulans* after CDC42 (*modA*) deletion, the mutant hyphae was broader and contained more nuclei than the wt. These phenotypes are similar to what we have observed in the Δ*rasA* mutant, and the increased number of nuclei may be a common response in mutants in which there is increased cytoplasmic volume and reduced hyphal extension, such as the *sepA1*, ΔCDC42, and Δ*rasA* mutants (11, 40). The Ras/Cdc42/MAPK pathway is likely a conserved module that functions in the regulation of hyphal growth in *A. fumigatus* and may be a downstream target of RasA activity. However, we saw no evidence of changes in transcript abundance in the Δ*rasA* mutant compared to the wt or the complemented strains (Fig. 9). This does not rule out regulation by translational or posttranslational mechanisms, which we are actively pursuing.

Deletion of *A. fumigatus rasA* led to an almost complete loss in conidiation that could be recovered by growth on osmotically stabilized medium (Table 3 and Fig. 3). Even though nearly wt levels of conidia were produced, microscopic observations of the conidiophores revealed that morphological abnormalities remained. The rudimentary conidiophores predominated, but even those that looked relatively normal showed blunted phialides and often were septate. The septated conidiophore stalks appeared to be stimulated in hyperosmotic medium, however, based on their increased frequency in the wt and Δ*rasA*+*rasA* strains (Fig. 4). Similar phenotypes have been reported in *A. nidulans*, in which expression of alleles carrying dominant-active or dominant-negative mutations of RasA leads to aberrant conidiophore morphology or cessation of the asexual developmental program, respectively (34). Another commonly reported phenotype of Ras mutants in fungi is the increased sensitivity to heat shock and/or high-temperature growth. Strains of *S. cerevisiae* and *C. albicans* expressing activated Ras alleles are hypersensitive to heat shock, whereas a *C. neoformans* Ras1 deletion strain displays reduced growth at elevated temperatures (1, 6, 13). Interestingly, the reduced growth phenotypes seen in the *A. fumigatus rasA* deletion mutant or in a strain expressing an activated allele were not related to the incubation temperature, at least under the conditions we examined. Perhaps this is because *A. fumigatus*, in contrast to the other fungi mentioned, is known to be thermotolerant, showing an optimal growth temperature of approxi-

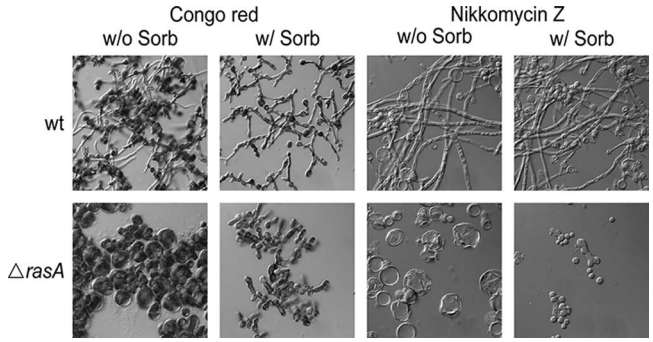

FIG. 7. Treatment of the *rasA* mutant with Congo red or Nikkomycin Z results in morphologically abnormal growth. Conidia (10^5) from the wt and Δ*rasA* strains were grown in AMM with the addition of 75 μg of Congo red or 1 μg of Nikkomycin Z/ml overnight at 37°C. Images are shown from cultures with (w/) or without (w/o) 1.2 M sorbitol (Sorb) added to the medium as an osmotic stabilizer.

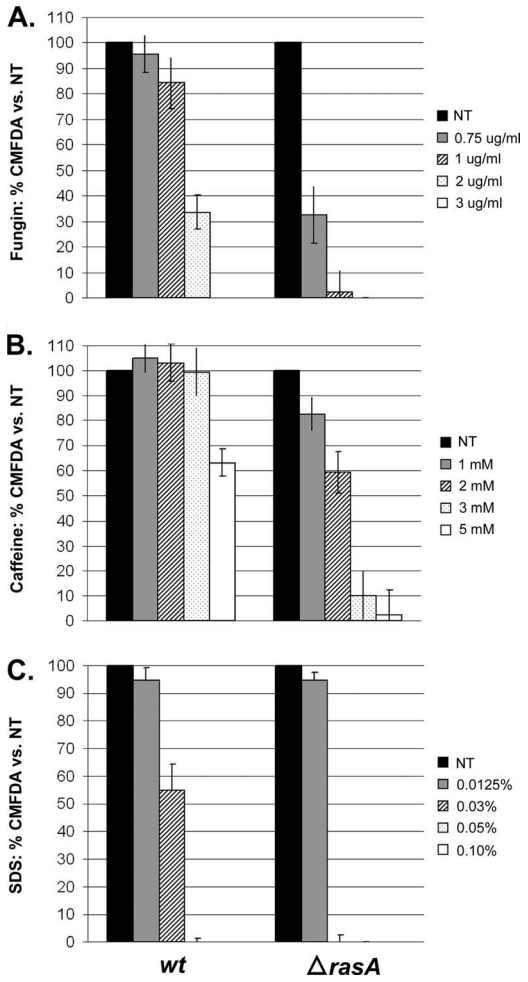

FIG. 8. The Δ*rasA* mutant is hypersensitive to cell wall stress. Fungal growth was measured using cleavage of CMFDA by strains treated with increasing concentrations of SDS (A), Fungin (B), and caffeine (C). All experiments were performed in triplicate. Measurements and error bars represent the mean ± the SD.

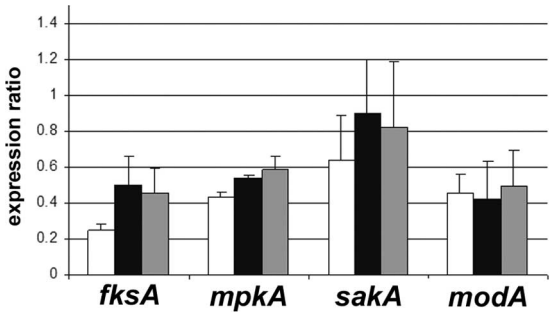

FIG. 9. Transcript abundance in members of the *rasA* isogenic set compared using RT-PCR. RNA from wt (□), Δ*rasA* (■), and Δ*rasA*+*rasA* (▨) was harvested from hyphae grown overnight as described in Materials and Methods. Products of the RT-PCR were run on gels and stained with Sybr green, and the intensity in pixels was normalized to the signal from *gpdA* run in the same gel. These ratios were then analyzed by analysis of variance, and no significant differences were detected.

mately 42°C. However, when taken together, these data indicate that many, but not all, of the reported *rasA* mutant phenotypes are conserved among the fungi.

The most surprising of the Δ*rasA* phenotypes revealed in the present study is the increased sensitivity noted when the mutant is grown in the presence of cell wall stressors: caffeine, used to test cell wall integrity in yeast; Congo red, an inhibitor of cell wall microfibril assembly; Nikkomycin Z, a chitin-synthase inhibitor; SDS, a detergent that disrupts the cell membrane; and Fungin, a polyene that disrupts ion exchange through the cell membrane. That the mutant might have abnormalities associated with its cell wall was first suggested by the difficulty in making protoplasts from the mutant when we were attempting to complement the mutation. The preparations used for protoplasting in *Aspergillus* are complex mixtures of various enzymes; most are culture filtrates, the components of which are not described in detail (Novozym 234) or are proprietary in nature (Vinoflow FCE). The combination of β-glucanase [which attacks the β-(1-4)-D-glucan linkages], lyticase [which hydrolyzes the β-(1-3)-D-glycopyranosyl linkages], and driselase (a crude powder containing laminarinase, xylanase, and cellulose) was not effective in digesting the cell walls from the Δ*rasA* mutant. Likewise, Vinoflow FCE, a proprietary mixture from Novozymes that is marketed as a wine maturation agent, was ineffective in making protoplasts. Only Novozym 234, a culture filtrate from *Trichoderma harzianum* reported to contain α-(1-3)-glucan glucanohydrolase and β-(1-3)-glucan glucanohydrolase, among other components, was able to make protoplasts readily from the Δ*rasA* mutant (5, 31). Because of the difficulty in making direct comparisons, either qualitative or quantitative, among the different protoplasting mixtures, we attempted to determine whether there were recognizable differences in cell wall composition or integrity that would help to explain our findings.

The cell wall integrity of the Δ*rasA* mutant was compared to the wt and reconstituted strains under stress induced by exposure to a known cell wall intercalating agent, a chitin synthase inhibitor, and cell membrane disruptors. The Δ*rasA* strain displayed decreased growth and/or abnormal morphology in the presence of all of the cell wall agents tested. In an effort to understand whether these phenotypes might be mechanistically related, we measured the β-glucan content of the cell walls, the transcript abundance of *fksA*, the β-glucan synthetase gene, and the integrity of the calcineurin signaling pathway, reasoning that that loss of cell wall integrity might be due to decreased structural β-glucan. Using aniline blue fluorescence, we were unable to detect any differences in β-glucan content among the members of the *rasA* isogenic set. Although the transcript level was somewhat elevated, rather than decreased as we had hypothesized, in the Δ*rasA* mutant, this increase was not significant. The calcineurin signaling protein, CnaA, has been shown to regulate β-glucan synthesis in *A. fumigatus*, and deletion of *rasA* results in phenotypes similar to those seen in the Δ*cnaA* mutant, including increased sensitivity to Nikkomycin Z (36). However, calcineurin signaling was still intact in the Δ*rasA* mutant, as displayed by continued sensitivity to cyclosporine (Fig. 3). These data indicate that the difference in susceptibility to cell wall perturbation in the mutant was not due to defective β-glucan biosynthesis and that RasA and CnaA may mediate their effects on cell wall integrity through distinct mechanisms.

Our second hypothesis was that RasA was upstream of MpkA, the cell wall integrity MAPK in *A. fumigatus* or, because of the effect of sorbitol on conidiation, of SakA, the Hog1 homolog (39, 43). Again, no significant differences in transcriptional abundance were detected (Fig. 9). Finally, since PKA signaling is involved in the general stress response in *S. cerevisiae* and in oxidative stress in *A. fumigatus*, the transcript levels of the genes encoding the PKA holoenzymes were examined and found to be equal in the isogenic set (10, 45). Therefore, although the cell wall integrity of the Δ*rasA* mutant was compromised, none of the pathways we investigated were involved via transcriptional mechanisms. However, this does not preclude regulation of the cell wall through other mechanisms.

In conclusion, the isolation of a complete *rasA* deletion mutant in *A. fumigatus* reported here is the first time such a deletion strategy has been successfully reported in a filamentous fungus. Deletion of *rasA* yielded some phenotypes that would be predicted, based on conserved Ras function among the fungi. These include decreased germination and growth rates, severely malformed hyphae with polarized growth defects, loss of conidiation, and abnormalities in nuclear distribution. Surprisingly, the Δ*rasA* strain demonstrated an intriguing phenotype of cell wall instability. This finding opens the exciting possibility of altering RasA activity, possibly through the use of farnesyl-transferase inhibitors, in combination with cell wall antifungals as a means of reducing *Aspergillus* viability. Future studies with the Δ*rasA* mutant will focus on defining the structure of the Δ*rasA* cell wall and delineating the pathways in which RasA acts to regulate asexual development and cell wall integrity.

ACKNOWLEDGMENTS

This study was supported by NIH grants AIO61497 (J.C.R.) and AI061495 (D.S.A.).

We thank Jay Card for his assistance with photography and figures.

REFERENCES

1. **Alspaugh, J. A., L. M. Cavallo, J. R. Perfect, and J. Heitman.** 2000. *RAS1* regulates filamentation, mating, and growth at high temperature of *Cryptococcus neoformans*. Mol. Microbiol. **36:**352–365.
2. **Boyce, K., M. Hynes, and A. Andrianopoulos.** 2005. The Ras and Rho GTPases genetically interact to co-ordinately regulate cell polarity during development in *Penicillium marneffei*. Mol. Microbiol. **55:**1487–1501.
3. **Cove, D. J.** 1966. The induction and repression of nitrate reductase in the fungus *Aspergillus nidulans*. Biochim. Biophys. Acta **113:**51–56.
4. **DaSilva-Ferreira, M., M. Kress, M. Savoldi, M. Goldman, A. Hartl, T. Heinekamp, A. Brakhage, and G. Goldman.** 2006. The *akuB* (KU80) mutant deficient for nonhomologous end joining is a powerful tool for analyzing pathogenicity in *Aspergillus fumigatus*. Eukaryot. Cell **5:**207–211.
5. **de la Cruz, J., J. Pintor-Toro, T. Benítez, and A. Llobell.** 1995. Purification and characterization of an endo-β-1,6-glucanase from *Trichoderma harzianum* that is related to its mycoparasitism. J. Bacteriol. **177:**1864–1871.
6. **Feng, Q., E. Summers, B. Guo, and G. Fink.** 1999. Ras signaling is required for serum-induced hyphal differentiation in *Candida albicans*. J. Bacteriol. **181:**6339–6346.
7. **Fillinger, S., M.-K. Chaveroche, K. Shimizu, N. Keller, and C. d'Enfert.** 2002. cAMP and ras signaling independently control spore germination in the filamentous fungus *Aspergillus nidulans*. Mol. Microbiol. **44:**1001–1016.
8. **Fortwendel, J. R., J. C. Panepinto, A. E. Seitz, D. S. Askew, and J. C. Rhodes.** 2004. *Aspergillus fumigatus rasA* and *rasB* regulate the timing and morphology of asexual development. Fungal Genet. Biol. **41:**129–139.
9. **Fukui, Y., T. Kozasa, Y. Kasiro, T. Takeda, and M. Yamamoto.** 1986. Role of a *ras* homolog in the life cycle of *Schizosaccharomyces pombe*. Cell **44:** 329–336.
10. **Godon, C., G. Lagniel, J. Lee, J.-M. Buhler, S. Kieffer, M. Perrot, H. Boucherie, M. B. Toledano, and J. Labarre.** 1998. The H2O2 stimulon in *Saccharomyces cerevisiae*. J. Biol. Chem. **273:**22480–22489.
11. **Harris, S., J. Morrell, and J. Hamer.** 1994. Identification and characterization of *Aspergillus nidulans* mutants defective in cytokinesis. Genetics **136:** 517–532.
12. **Herman, P. K., and J. Rhine.** 1997. Yeast spore germination: a requirement for Ras protein activity during re-entry into the cell cycle. EMBO J. **16:**6171–6181.
13. **Jiang, Y., C. Davis, and J. R. Broach.** 1998. Efficient transition to growth on fermentable carbon sources in *Saccharomyces cerevisiae* requires signaling through the Ras pathway. EMBO J. **17:**6942–6951.
14. **Kataoka, T., S. Powers, C. McGill, O. Fasnao, J. Strathern, J. Broach, and M. Wigler.** 1984. Genetic analysis of yeast *RAS1* and *RAS2* genes. Cell **37:**437–445.
15. **Ko, Y.-T., and Y.-L. Lin.** 2004. 1,3-β-Glucan quantification by a fluorescence microassay and analysis of its distribution in foods. J. Agric. Food Chem. **52:**3313–3318.
16. **Latge, J.-P.** 1999. *Aspergillus fumigatus* and aspergillosis. Clin. Microbiol. Rev. **12:**310–350.
17. **Leberer, E., D. Harcus, D. Dignard, L. Johnson, S. Ushinsky, D. Y. Thomas, and K. Schroppel.** 2001. Ras links cellular morphogenesis to virulence by regulation of the MAP kinase and cAMP signaling pathways in the pathogenic fungus *Candida albicans*. Mol. Microbiol. **42:**673–687.
18. **Lee, N., and J. W. Kronstad.** 2002. *ras2* controls morphogenesis, phermone response, and pathogenicity in the fungal pathogen *Ustilago maydis*. Eukaryot. Cell **1:**954–966.
19. **Lengeler, K. B., R. C. Davidson, C. D'souza, T. Harashima, W.-C. Shen, P. Wang, X. Pan, M. Waugh, and J. Heitman.** 2000. Signal transduction cascades regulating fungal development and virulence. Microbiol. Mol. Biol. Rev. **64:**746–785.
20. **Maschmeyer, G., A. Haas, and O. A. Cornely.** 2007. Invasive aspergillosis: epidemiology, diagnosis and management in immunocompromised patients. Drugs **67:**1567–1601.
21. **Momany, M., and I. Taylor.** 2000. Landmarks in the early duplication cycles of *Aspergillus fumigatus* and *Aspergillus nidulans*: polarity, germ tube emergence, and septation. Microbiology **146:**3279–3284.
22. **Mosch, H. U., E. Kubler, S. Krappmann, G. F. Fink, and G. H. Braus.** 1999. Crosstalk between the Ras2p-controlled mitogen-activated protein kinase and cAMP pathways during invasive growth of *Saccharomyces cerevisiae*. Mol. Biol. Cell **10:**1325–1335.
23. **Nikawa, J., S. Cameron, T. Toda, K. M. Ferguson, and M. Wigler.** 1987. Rigorous feedback control of cAMP levels in *Saccharomyces cerevisiae*. Genes Dev. **1:**931–937.
24. **Oliver, B. G., J. C. Panepinto, D. S. Askew, and J. C. Rhodes.** 2002. cAMP alteration of growth rate of *Aspergillus fumigatus* and *Aspergillus niger* is carbon-source dependent. Microbiology **148:**2627–2633.
25. **Osherov, N., and G. May.** 2000. Conidial germination in *Aspergillus nidulans* requires Ras signaling and protein synthesis. Genetics **155:**647–656.
26. **Ovechkina, Y. Y., R. K. Pettit, Z. A. Cichacz, G. R. Pettit, and B. R. Oakley.** 1999. Unusual antimicrotubule activity of the antifungal agent spongistatin 1. Antimicrob. Agents Chemother. **43:**1993–1999.
27. **Panepinto, J. C., B. G. Oliver, T. W. Amlung, D. S. Askew, and J. C. Rhodes.** 2002. Expression of the *Aspergillus fumigatus rheB* homologue, *rhbA*, is induced by nitrogen starvation. Fungal Genet. Biol. **36:**207–214.
28. **Papadaki, P., V. Pizon, B. Onken, and E. C. Chang.** 2002. Two ras pathways in fission yeast are differentially regulated by two ras guanine exchange factors. Mol. Cell. Biol. **22:**4598–4606.
29. **Pichova, A., D. Vondrakova, and M. Breitenbach.** 1997. Mutants in the *Saccharomyces cerevisiae RAS2* gene influence life span, cytoskeleton, and regulation of mitosis. Can. J. Microbiol. **43:**774–781.
30. **Punt, P. J., R. P. Oliver, M. A. Dingemanse, P. H. Pouwels, and C. A. v. d. Hondel.** 1987. Transformation of *Aspergillus* based on the hygromycin B resistance marker from *Escherichia coli*. Gene **56:**117–124.
31. **Rhodes, J., and K.-J. Kwon-Chung.** 1985. Production and regeneration of protoplasts from *Cryptococcus*. Sabouraudia J. Med. Vet. Mycol. **23:**77–80.
32. **Roberts, R. L., H. U. Mosch, and G. R. Fink.** 1997. 14-3-3 proteins are essential for RAS/MAPK cascade signaling during pseudohyphal development in *Saccharomyces cerevisiae*. Cell **89:**1055–1065.
33. **Shedletzky, E., C. Unger, and D. P. Delmer.** 1997. A microtiter-based fluorescence assay for (1,3)-beta-glucan synthases. Anal. Biochem. **249:**88–93.
34. **Som, T., and V. S. R. Kolaparthi.** 1994. Developmental decisions in *Aspergillus nidulans* are modulated by Ras activity. Mol. Cell. Biol. **14:**5333–5348.
35. **Steinbach, W., J. R. A. Cramer, B. Perfect, Y. Asfaw, T. Sauer, L. Najvar, W. Kirkpatrick, T. Patterson, J. DK Henderson, J. Heitman, and J. Perfect.** 2006. Calcineurin controls growth, morphology, and pathogenicity in *Aspergillus fumigatus*. Eukaryot. Cell **5:**1091–1103.
36. **Steinbach, W., J. R. A. Cramer, B. Perfect, C. Henn, K. Nielsen, J. Heitman, and J. Perfect.** 2007. Calcineurin inhibition or mutation enhances cell wall inhibitors against *Aspergillus fumigatus*. Antimicrob. Agents Chemother. **51:** 2979–2981.
37. **Toda, T., I. Uno, T. Ishikawa, S. Powers, T. Kataoka, D. Broek, S. Cameron, J. Broach, K. Matsumoto, and M. Wigler.** 1985. In yeast, RAS proteins are controlling elements of adenylate cyclase. Cell **40:**27–36.
38. **Truesdell, G., C. Jones, T. Holt, G. Henderson, and M. Dickman.** 1999. A Ras protein from a phytopathogenic fungus causes defects in hyphal growth polarity, and induces tumors in mice. Mol. Gen. Genet. **262:**46–54.
39. **Valiante, V., T. Heinekamp, R. Jain, A. Hartl, and A. A. Brakhage.** 2008. The mitogen-activated protein kinase MpkA of *Aspergillus fumigatus* regulates cell wall signaling and oxidative stress response. Fungal Genet. Biol. **45:**618–627.
40. **Virag, A., M. P. Lee, H. Si, and S. D. Harris.** 2007. Regulation of hyphal morphogenesis by *cdc42* and *rac1* homologues in *Aspergillus nidulans*. Mol. Microbiol. **66:**1579–1596.
41. **Weeks, G., and G. B. Spiegelman.** 2003. Roles played by Ras subfamily proteins in the cell and developmental biology of microorganisms. Cell Signal **15:**901–909.
42. **Wendland, J., and P. Philippsen.** 2001. Cell polarity and hyphal morphogenesis are controlled by multiple rho-protein modules in the filamentous ascomycete *Ashbya gossypii*. Genetics **157:**601–610.
43. **Xue, T., C. K. Nguyen, A. Romans, and G. S. May.** 2004. A mitogen-activated protein kinase that senses nitrogen regulates conidial germination and growth in *Aspergillus fumigatus*. Eukaryot. Cell **3:**557–560.
44. **Zarember, K. A., J. A. Sugui, Y. C. Chang, K. J. Kwon-Chung, and J. I. Gallin.** 2007. Human polymorphonuclear leukocytes inhibit *Aspergillus fumigatus* conidial growth by lactoferrin-mediated iron depletion. J. Immunol. **178:**6367–6373.
45. **Zhao, W., J. Panepinto, J. Fortwendel, L. Fox, B. Oliver, D. Askew, and J. Rhodes.** 2006. Deletion of the regulatory subunit of protein kinase A in *Aspergillus fumigatus* alters morphology, sensitivity to oxidative damage, and virulence. Infect. Immun. **74:**4865–4874.